Behaviour of Over-reinforced High-Strength Concrete Beams Confined with Post-Tensioned Steel Straps: an experimental investigation

Chau-Khun Ma[a*], Abdullah Zawawi Awang[a], Reyes Garcia[b], Wahid Omar[a], Kypros Pilakoutas[b]

[a] *Faculty of Civil Engineering, Universiti Teknologi Malaysia, 81310, Skudai, Johor, Malaysia.*

[b] *Dept. of Civil and Structural Engineering, The University of Sheffield, Sir Frederick Mappin Building, Mappin Street, Sheffield, S1 3JD, UK.*

Tel: +6016-8366360

Email (corresponding author*): machaukhun@gmail.com

Abstract

This study examines the flexural behaviour of High-Strength Concrete (HSC) beams confined using an innovative Steel Strapping Tensioning Technique (SSTT) able to provide active confinement. Twelve over-reinforced HSC beams (f_c=50 or 80 MPa) were designed to fail prematurely by concrete crushing at midspan. The midspan of eight of such beams was confined externally using the SSTT with different steel strap confinement ratios, which aimed to delay concrete crushing. The test results are discussed in terms of the failure modes, load-deflection response, and observed concrete and tensile reinforcement strains. Whilst unconfined beams failed in a brittle manner with no post-peak deflection, the steel straps were very effective at enhancing the post-peak deformation of the SSTT-confined beams by up to 126%. Moreover, for the beams tested in this study, the use of the SSTT led to failures after yielding of the tensile reinforcement. The proposed SSTT can be used to confine HSC elements where ductility is required.

Keywords: Beams, High-Strength Concrete; Steel Straps; Active Confinement; Post-peak Deflections

1. Introduction

In the last two decades, the use of high-strength concrete (HSC) in construction has increased considerably due to its higher load-carrying capacity and stiffness compared to normal-strength concrete (NSC). Moreover, structural elements designed with HSC are usually smaller, which may lead to lower overall construction costs. However, the axial stress-strain relationship of HSC generally exhibits a steeper and shorter descending post-peak branch compared to NSC, which in turn reduces the ultimate (post-elastic) strain of concrete. The lower deformability capacity of HSC may lead to potential brittle failures in structural elements with light confinement and, as a result, HSC is more commonly used in structures that need to develop low ductility (e.g. high-rise buildings or long-span bridges located in non-seismic regions). In order to use HSC in structures located in seismic regions, it is necessary to develop more practical, efficient and cost-effective confining methods.

Recently, an innovative "active confining" technique (referred hereafter as Steel Strapping Tensioning Technique, or SSTT) has proven very effective at enhancing the capacity and ultimate strain of small-scale HSC cylinders [1], thus preventing brittle failure of the cylinders. The SSTT involves the post-tensioning of high-strength steel straps around RC members using air-operated strapping tools as those utilised in the packaging industry. Following the post-tensioning, the steel straps are clamped mechanically using self-regulated end clips to maintain the tensioning force. Unlike other confining techniques (e.g. the use of internal stirrups or external FRP wraps), the external strapping provides active confinement to the full cross-section of members, thus increasing their ductility and capacity. The SSTT has other advantages such as ease and speed of application, ease of removing or replacing steel straps, and lower material and labour costs. Previous experimental research utilised the SSTT as a confining solution for larger-scale columns cast with NSC [2] and HSC [3], but the use of the SSTT on other common HSC elements that need to develop significant levels of ductility (e.g. beams subjected to bending) needs to be investigated.

The behaviour of RC beams subjected to flexure mainly depends on the beams' failure mode, which in turn depends on the amount of tensile (bottom) steel reinforcement provided to the beam [4]. When subjected to flexure, under-reinforced beams with less tensile reinforcement than that corresponding to the "balanced condition" will fail in a ductile manner by yielding of such reinforcement, but before the compressed concrete reaches its maximum strain. Conversely, over-reinforced beams with more tensile reinforcement than the “balanced condition” will fail in a brittle manner by concrete crushing. To prevent such undesirable sudden failure, current design codes limit the tension reinforcement ratio (e.g. ACI 318, [5]) or the neutral axis depth (e.g. Eurocode 2, [6]) to ensure that all beams are under-reinforced and therefore able to develop a minimum level of ductility. However, designing RC beams to be under-reinforced also prevents the full utilisation of the enhanced material properties that HSC can potentially provide. Moreover, the use of confinement can delay the failure of the compressed HSC concrete so that the tensile reinforcement yields before the concrete crushes. Whilst previous studies have examined the effectiveness of internal steel stirrups (i.e. passive confinement) at enhancing the flexural ductility of HSC beams ([7], [8], [9], [10]), to date no experimental research has investigated the feasibility of using external active confinement (e.g. SSTT) on such structural elements.

This article examines experimentally the influence of the SSTT on the behaviour of over-reinforced HSC beams tested in four-point bending. To investigate the effect of external active confinement on the concrete crushing at the compressed zone, the midspan of the beams is confined using the SSTT, which is expected to increase the ultimate strain of the HSC and thus the deformation capacity of the beams. The results are discussed in terms of the observed failure modes and load-deflection curves, as well as concrete and tensile reinforcement strains observed during the tests.

2. Experimental methodology

2.1 Characteristics of tested beams

The twelve tested beams had a rectangular cross section of 100×200 mm and a total length of 2400 mm, as shown in Figure 1. To examine different flexural reinforcement ratios, the main flexural reinforcement of six beams (Type 1 shown in Figure 1a) consisted of 2Ø10mm+2Ø12mm longitudinal bars, whereas the reinforcement of another six beams (Type 2, Figure 1b) consisted of 2Ø8mm+2Ø16mm bars. The above number of bars produced tensile reinforcement ratios of 0.0306 to 0.0447, i.e. +3% to +50% of the balanced reinforcement ratio ρ_b=0.0298. No transverse internal reinforcement (stirrups) was provided to the beams Type 1. For beams Type 2, 6 mm fully closed stirrups were provided along the beam length but not at midspan (Figure 1b). These stirrups were held in place using 6 mm bars used as top reinforcement (Figure 1d). For all beams, the free concrete cover to the longitudinal reinforcement was 20 mm (Figure 1e).

2.2 Material properties

Beams Type 1 were cast using two batches of HSC, whereas another two batches were used to cast the beams Type 2. The target mean concrete compressive strengths for beam Types 1 and 2 were f_c=50 and 80 MPa, respectively. After casting, the beams were covered with polythene sheets and wet hessian, cured for two days in the moulds and subsequently stored under standard laboratory conditions until testing. The mean concrete compressive strength of each batch was obtained from tests on three 100×200 mm concrete cylinders according to ASTM C39/C39M [11]. Table 1 reports the average results and standard deviations (SD) from the tests on cylinders.

The main bottom reinforcement of the beams consisted of high ductility ribbed bars complying with ASTM A615 [12]. The mechanical properties of the bars were obtained by testing three bar samples in direct tension and the results are reported in Table 2. The elastic modulus of all bars was E_s=205 GPa. Commercially available high-strength steel straps with nominal cross section 0.52×15mm and corrosion-resistant surface coating were used as external confinement. These straps are typically used in the packaging industry in Southeast Asia. Table 2 shows the mechanical properties of the steel straps obtained from three sample coupon tests.

2.3 Confinement of beams with the SSTT

Eight beams (four Type 1 and four Type 2) were confined along their full length using the SSTT. The number and spacing of steel straps selected for these tests aimed to produce modest values of volumetric confinement ratios ρ_v ($\rho_v = V_s f_{ys}/V_c f_c$, where V_s and V_c are the volumes of straps and confined concrete, respectively, and f_{ys} is the yield strength of the straps). For beams Type 1, the clear spacing s_c between straps was either 20 mm or 40 mm, thus leading to volumetric confinement ratios ρ_v of 0.089 and 0.146, respectively. The spacing selected for beams Type 2 (s_c=15 or 30 mm) produced values ρ_v of 0.066 and 0.104, respectively. In actual confinement applications designers are free to select the volumetric ratio ρ_v by changing the strap spacing, number of strap layers, yield strength of the straps and compressive concrete strength. However, typical values of ρ_v for practical confining applications on HSC elements range between 0.05 and 0.50 [1]. Four unconfined control beams were also tested for comparison purposes. The specimens are identified according to the target concrete strength (50 or 80 MPa), beam Type (either 1 or 2), and clear spacing between steel straps (20 or 40 mm, and 15 or 30 mm). For example, B80-1-15 refers to a beam Type 1 with a concrete compressive strength of 80 MPa, and with a strap spacing of 15 mm. In the case of the control specimens (no external steel strapping), a letter "C" replaces the last two digits. Figure 2 shows a typical beam externally confined with the SSTT. All straps were post-tensioned using a compressed-air strapping tool set to an initial pressure of

2.0 bar, which led to a tensioning force in the straps of approximately 10-15% of their yield strength. Most air tools using portable air compressors operate at pressures of 5-6 bar and therefore the proposed technique can be easily used in practice. To maintain the post-tensioning force, the straps were fastened mechanically using self-regulated end clips (shown in Figure 3). It should be mentioned that, during strap post-tensioning, some stress losses are expected in the straps due to friction between the straps and the concrete surface. However, previous test results [13] indicate that the stress reduction due to friction is negligible (usually less than 10%). Table 3 summarises the characteristics of the beams tested in this study.

2.4 Test set-up and instrumentation

All beams were tested in four-point bending to produce a constant moment (and eventually failure) over the midspan region, as shown in Figure 4. The load from the vertical jack was applied symmetrically through a stiff spreader loading beam. The beams were simply supported over a clear span of 2200 mm. Three linear transducers measured vertical deflections: one at the midspan, and two located at 300 mm from the centerline of the beam (see Figure 4). Four 60 mm electrical resistance strain gauges were fixed horizontally on the beams' face (between loading points) to monitor the concrete compressive strains over the beams' depth. 30 mm gauges were fixed on the longitudinal tensile reinforcement and on the steel straps (after tensioning) at midspan to measure strains during the tests. All data were recorded by a data logger. The formation and development of cracks was visually monitored and marked on the white-washed faces of the beams by stopping the applied load at approximate intervals of 2.0 kN. This also allowed recording the onset of flexural cracking when the first flexural crack was observed at midspan in between the applied loads. The tests were halted when the brittle failure of the beams occurred (unconfined control specimens), or when the peak load capacity of the beam dropped by 20% (SSTT-confined beams).

3. Experimental results and discussion

Table 4 reports the following results for the tested beams: a) load at onset of flexural cracking, b) peak load P_{max}, b) midspan deflection δ at P_{max}, c) enhancements of peak load ΔP_{max} and midspan deflection $\Delta\delta$ of SSTT-confined beams over unconfined control specimens, d) post-peak midspan deflection δ_{-20} after a 20% drop of P_{max}, e) ratio of deflections δ_{-20}/δ, f) ultimate concrete strain at beam failure recorded by the strain gauges, g) flexural reinforcement strain at beam failure, h) steel strap strains at beam failure, i) number of cracks and average crack spacing measured after the tests and j) estimated ultimate load using CEN (2004). The following section discusses the results reported in Table 4 and summarises the most significant observations of the experimental programme.

3.1 Failure modes

The onset of flexural cracking in beams B50 and B80 occurred within the midspan region at approximate loads of 10.0 and 8.0 kN, respectively (see Table 4). As the load increased, the length of flexural cracks at midspan extended, whereas additional flexural cracks developed outside the midspan zone. As a consequence of significant compression, concrete 'flaking off' was observed at the top of the beams' midspan as the load was reaching its peak value. As expected, the unconfined control beams failed in a sudden and brittle manner due to crushing of the (top) concrete at the midspan. This was accompanied by the sudden formation of additional diagonal cracks towards the beam supports, which in turn produced spalling of the concrete cover at the soffit of beams B50-1-C and B80-1-C. Figure 5a-b show typical failures of the unconfined beams B50 and B80. Whilst the straps apply compressive stresses mainly at the corners of the beams' cross section, no concrete cracking was evident at such locations during the tests.

As expected, the use of SSTT confinement at the beams' midspan did not modify considerably the onset of flexural cracking. However, specimens B50-2-20 and B80-1-30 experienced premature onset of flexural cracking when compared to their control specimen (see Table 4). These results can be attributed to the relatively high variability of concrete in tension, which may have caused early cracking in such beams compared to the control counterparts.

The experimental observations indicate that, unlike the unconfined control counterparts, the use of the SSTT prevented the brittle failure of the specimens. Concrete flaking off was only observed at zones of the midspan in between confining straps. Additionally, the steel straps fixed outside the midspan contributed to preventing the concrete cover spalling observed at the soffit of the control beams B50-1-C and B80-1-C. Overall, fewer cracks were observed in the SSTT-confined beams compared to the unconfined beams (see Table 4). The data in Table 4 also indicate that (measured) crack spacing increased in all SSTT-confined beams. Whilst the use of the SSTT at midspan aimed at increasing the ultimate strain capacity of the HSC in compression, the experimental observations indicate that the active confinement influenced crack development at the tension zone by a) enhancing the bond-slip behaviour of the flexural reinforcing bars, and b) strengthening weak sections of concrete subjected to tension, thus forcing cracks to form between straps where concrete may have been slightly stronger. However, further research is necessary to investigate the effect of SSTT on concrete crack development of RC members. Figure 7 shows typical failures experienced by the SSTT-confined beams. It is shown that the proposed SSTT confining technique was very effective at maintaining the integrity of the beams even after concrete crushing.

The change of failure mode of the SSTT-confined beams can be explained as follows. In members subjected to pure flexure (especially over-reinforced beams), the compression zone is relatively small compared to the tension zone [14]. Therefore, the lateral dilation of the compressed concrete is negligible and any confining effect is small. Nonetheless, the confinement maintains the concrete strains low and delays the formation of micro-cracking. As more energy is required during the test to increase the strain in the tensile reinforcement to achieve the balanced condition, the neutral axis moves upwards, thus leading to less brittle failures (see Figure 7). Since the confinement delayed the formation of micro-cracking and increased the concrete strain capacity in compression, yielding of the tensile reinforcement occurred prior to the failure of the concrete in compression, as described in a following section. Consequently, the original over-reinforced HSC beams (with shallow neutral axis) failed in a less brittle manner when using the SSTT at the midspan.

3.2 Load-deflection relationships

Figure 8a-d compare the load-midspan deflection responses of the tested specimens, where the sudden failure of the unconfined control beams is indicated using a star symbol. Comparatively, the use of external SSTT confinement led to 'ductile' responses, characterised by a gentle drop of the capacity after the peak load. The minor differences in the load-deflection curves of beams in the same plot can be attributed to the slightly different cross section dimensions among specimens, which was unavoidable during casting.

Figure 8a-b show that the control beams B50-1-C and B50-2-C failed at a peak load of 46.0 and 36.0 kN, respectively, and sustained deflections δ of only 23 mm. Figure 8a-b and the data in Table 4 indicate that the SSTT was very effective at enhancing the load-deflection behaviour of the beams. The capacity of beams B50 was enhanced by a minimum of 7% (B50-1-40) and up to 22% (B50-2-20 and B50-2-40) over their unconfined control counterparts. Moreover, compared to their corresponding unconfined beams, the deflection δ of the SSTT-confined beams was enhanced by a minimum of 20% (B50-2-40) and up to 41% (B50-1-40).

Figure 8c-d and Table 4 also show that the capacity of the SSTT-confined beams B80-1-15 and B80-1-30 was 8% and 6% higher than that of the control beam B80-1-C. Nonetheless, the SSTT-confined beams B80-2-15 and B80-2-30 had a slightly lower capacity (up to -5%) when compared to the corresponding unconfined beam B80-2-C. This is due to the unusually slightly larger capacity resisted by the latter specimen, which can be attributed to minor variations in the effective dimensions and position of flexural bars in this beam. Nonetheless, with the exception of beam B80-2-15, the use of SSTT confinement consistently enhanced the deflection δ of beams B80 by up 39% (see B80-1-15). The effectiveness of the external confinement is further evidenced by considering the post-peak deflections. Even after a drop of 20% in peak load, the δ_{-20}/δ ratios of all SSTT-confined beams show that the post-deflection δ_{-20} increased by minimum 20% (B80-1-30) and up to 126% (B50-2-20). As expected, the beams with heavier external SSTT confinement (s_c=20 and 15 mm) sustained larger deflections δ_{-20} compared to similar beams with lighter confinement (s_c=40 and 30 mm). Also, the use of the internal steel stirrups in beams B50-2 and B80-2 has negligible effect on the load-deflection response of the beams, as such stirrups were mainly used to prevent shear failures outside the midspan region of beams Type 2. Overall, the experimental results indicate that even small amounts of SSTT confinement are sufficient to prevent brittle failure of the concrete at the beams' midspan, which in turn gives considerable post-peak deformation capacity.

Table 4 also compares the capacity of each tested beam with the theoretical capacity of an equivalent beam confined with conventional internal steel stirrups. The theoretical capacity of the latter beam ($P_{max,t}$) was calculated using the *fib* Model Code [15] assuming that the steel stirrups of the equivalent beams had a diameter of 6 mm and a yield strength of f_y=250 MPa (mild steel is assumed). The spacing of the internal stirrups of the equivalent beams was also assumed to be equal to the spacing of steel straps of the SSTT-confined beams. For example, the spacing of stirrups for the equivalent beam of the tested specimen ‘B50-1-20’ was assumed as 20 mm. For a similar stirrup spacing, Table 4 shows that the capacity enhancement $\Delta P_{max,t}$ of the beams confined with internal stirrups over the corresponding unconfined theoretical beams is only 1-5%, i.e. significantly lower than that achieved using the steel straps. However, it should also be also noted that the capacity enhancement of the confined beams could be due to experimental scatter as only one sample was tested for each combination of parameters, and therefore further tests are necessary to eliminate the concrete strength variability. Nonetheless, the overall trends observed in the results of the SSTT-confined beams indicate improvements in load and deformation capacity, thus opening the way of using SSTT in new applications in the construction industry.

3.4 Load-flexural reinforcement strain curves

Figure 9 shows the load-strain curves for the flexural reinforcement of beams B50-2. These are typical results and the following observations apply to the rest of the beams. As expected, the over-reinforced control beams with no midspan confinement (star symbol in Figure 9) failed just before or immediately after the onset flexural bar yielding, as confirmed by the steel strains reported in Table 2. Comparatively and regardless of the concrete strength or steel strap confinement ratio, the flexural reinforcement of all SSTT-confined specimens developed some yielding as indicated by short post-yield plateaus in Figure 9a-d (except for beam B50-2-20). As such, the SSTT confinement was effective at achieving bar yielding in regardless of the flexural reinforcement ratio used in these beams. However, as mentioned previously, ultimate failure mode of the beams was dominated by concrete crushing at midspan.

The data in Table 4 also indicate that the straps fixed at midspan of all SSTT-confined beams remained within the elastic range. A close inspection at the end of the tests revealed that most of the straps maintained their initial tensioning force. However, additional tests are necessary to examine the long-term behaviour of the SSTT.

3.5 Load-concrete strain curves

Figure 10a-b compares the concrete compressive strains recorded by the top gauge fixed on the beams´ faces. In these plots, the failure of the unconfined control beams is represented using stars. Unfortunately, the strain gauge of the SSTT-confined beam B50-1-C detached prematurely as it was subjected to excessive compression. As a result, the effectiveness of the SSTT at enhancing the ultimate concrete strain in beams B50-1 cannot be assessed. However, the results for beams B50-2, B80-1 and B80-2 indicate that the use of SSTT enhanced the ultimate concrete compressive strains (at beam failure) by up to 68% (see beam B80-2-30). These results can be justified by analysing the way HSC crushes in compression, which is captured by its uniaxial stress-strain relationship. Initially, concrete expands laterally due to a relatively constant Poisson's ratio (0.15-0.20). The Poisson's ratio increases marginally with the stress as microcracks develop due to lateral strain. Just before 85% of its capacity, concrete starts to crack laterally and the apparent Poisson's ratio increases rapidly, leading to larger lateral strains and peak axial load. The unstable initiation of lateral cracking leads to the compressive failure of HSC concrete, which loses rapidly strength in an uncontrolled manner and leads to small failure strains in the axial direction. The active confinement provided by the SSTT limits the lateral cracking of concrete, which in turn increases its compressive strength and its capacity to undergo larger ultimate compressive strains in the axial direction.

Based on the results of this study, it is concluded that the SSTT as external confinement is a very effective solution to increase the ultimate concrete compressive strains of over-reinforced HSC beams. Considering that the deformation capacity of over-reinforced RC elements depends primarily on the ultimate capacity of the concrete in compression (i.e. that the deformation of over-reinforced elements depends on the 'ductile' capacity of concrete), the results of this study indicate that larger deformation capacity can be expected in SSTT-confined HSC elements than in unconfined elements. Indeed, the use of the SSTT enhanced the compressive strain of concrete so that sudden explosive failure (generally observed in HSC elements) was delayed. However, further tests are necessary to investigate the use of heavier confinement (ρ_v>0.2) on the ultimate strain of other HSC elements.

4. Summary and conclusions

Twelve over-reinforced HSC beams were designed to fail prematurely by concrete crushing at midspan when tested in flexure. The midspan of eight of such beams was confined externally using a novel steel-strapping tensioning technique (SSTT) able to provide active confinement. Different steel strap confinement ratios were selected to delay concrete crushing so as to increase the load and deflection capacities of the beams. Based on the results of this study, the following conclusions can be drawn:

1) Over-reinforced unconfined control beams failed in a brittle manner due to concrete crushing at midspan. After failure, the beams were not able to sustain additional deformations.
2) In comparison to unconfined specimens, SSTT-confined beams failed at higher loads (by up to 22%) and deflections at peak load (by up 41%). After the peak load, SSTT-confined beams sustained significant post-peak deformations accompanied by a gradual drop in capacity. As expected, the use of heavier confinement (strap spacing s_c=20 and 15 mm) led to larger post-peak deflection capacities. Nonetheless, the final failure mode of the confined beams was dominated by concrete crushing at midspan.
3) Whilst the unconfined control beams failed just before or immediately after the onset flexural bar yielding, the flexural reinforcement of the SSTT-confined specimens

developed some yielding. This indicates that even modest amounts of external SSTT confinement (ρ_v=0.089-0.146) were sufficient to develop some ductility in the beams.

4) Overall, the test results indicate that the use of SSTT enhanced the ultimate concrete compressive strains (at beam failure) by up to 68%. Moreover, the proposed SSTT confining technique was very effective at maintaining the integrity of the beams even after concrete crushing.

Notation

f_c	concrete compressive strength
f_y	yield strength of flexural reinforcement
f_{ys}	yield strength of steel straps
f_u	ultimate strength of flexural reinforcement or steel straps
ε_y	yield strain of flexural reinforcement or steel straps
ε_u	ultimate strain of flexural reinforcement or steel straps
E_s	elastic modulus of flexural reinforcement or steel straps
ρ_v	volumetric confinement ratio
V_s	volume of confining steel straps
V_c	volume of confined concrete
s_c	clear spacing between confining steel straps
P_{max}	peak load resisted by a beam
δ	midspan deflection at peak load P_{max}
ΔP_{max}	enhancement of peak load of SSTT-confined beams over control beam
$\Delta\delta$	enhancement of midspan deflection of SSTT-confined beams over control beam
δ_{-20}	post-peak midspan deflection after a 20% drop of P_{max}

References

[1] *Lee, H.P., Awang, A.Z., Omar, W.*: Steel strap confined high strength concrete under uniaxial cyclic compression. Construction and Building Materials, vol. 72, 2014, pp. 48-55.

[2] *Garcia, R., Hajirasouliha, I., Guadagnini, M., Helal, Y., Jemaa, Y., Pilakoutas, K., Mongabure, P., Chrysostomou, C., Kyriakides, N., Ilki, A., Budescu, M., Taranu, N., Ciupala, M.A., Torres, L., Saiidi, M.*: Full-scale shaking table tests on a substandard RC building repaired and strengthened with Post-Tensioned Metal Straps. Journal of Earthquake Engineering, vol. 18, No. 2, 2014, pp.187-213.

[3] *Ma, C.K., Awang, A.Z., Omar, W., Maybelle, L.*: Experimental tests on SSTT-confined HSC columns. Magazine of Concrete Research, vol. 66, No. 21, 2014, pp. 1084-1094.

[4] *Jeffry, R., Hadi, M.N.S.*: The effect of confinement shapes on over-reinforced HSC beams. Proceedings of World Academy of Science, Engineering and Technology, vol. 30, No. 4, 2008, pp. 260-267.

[5] ACI Committee 318: Building code requirements for reinforced concrete. American Concrete Institute, Farmington Hills, MI, 2011.

[6] CEN: Eurocode 2: Design of concrete structures, Part 1- General rules and rules for building. European Committee for Standardisation, Brussels, 2004.

[7] *Mansur, M.A., Chin, M.S., Wee, T.H.*: Flexural behavior of high-strength concrete beams. ACI Structural Journal, vol. 94, No. 6, 1997, pp. 663-674.

[8] *Pinto, D.G., Bernardo, L.F.A., de Oliveira, L.A.P.*: Influence of Confinement with Transverse Reinforcement on the Flexural Ductility of High-Strength Concrete Beams. In: II Ibero-American Symposium on Concrete for Structures (INCOS2006), Rio de Janeiro, Brazil, September, 2006.

[9] *Bernardo, L.F.A., Oliveira, L.A.P., Pinto, D.G.*: Influence of transversal reinforcement on plastic rotation capacity of high-strength beams. ACI Special Publication, vol. 253, 2008, pp. 305-322.

[10] *Li-Young, J., Hoon-Gyu, P., Yong-Gon, K., Sung-Soo, K., Jong-Hoe, K.*: Flexural behavior of high-strength concrete beams confined with stirrups in pure bending zone. International Journal of Concrete Structures and Materials, vol.3, No.1, 2009, pp. 39-45.

[11] ASTM 39/39M-14a: Standard Test Method for Compressive Strength of Cylindrical Concrete Specimens. ASTM International, Barr Harbor Drive, West Conshohocken, PA, 2014.

[12] ASTM A615/A615M-14: Standard Specification for Deformed and Plain Carbon-Steel Bars for Concrete Reinforcement. ASTM International, Barr Harbor Drive, West Conshohocken, PA, 2014.

[13] *Moghaddam, H., Samadi, M., Pilakoutas, K., Mohebbi, S.*: Axial compressive behavior of concrete actively confined by metal strips, part A: experimental study. Materials and Structures, vol. 43, No. 10, 2010, pp.1369-1381.

[14] *Achintha, P.M.M., Burgoyne, C.J.*: Moment-curvature and strain energy of beams with external fiber-reinforced polymer reinforcement. ACI Structural Journal, vol. 106, No. 1, 2009, pp. 20-29.

[15] *fib*: Model Code for Concrete Structures 2010. 1st Edn. Ernst & Sohn GmbH & Co, Berlin, Germany, 2013.

Tables

Table 1 Properties of concrete at 28 days used to cast the beams

		Beams Type 1		**Beams Type 2**	
		Batch 1	Batch 2	Batch 1	Batch 2
Compressive strength, f_c (MPa)	Mean	54.5	51.1	79.6	78.8
	SD	2.31	0.57	3.44	2.10

Table 2 Average mechanical properties of reinforcing bars and metal straps

Nominal diameter (mm)	**6**	**8**	**10**	**12**	**16**	**Steel straps 0.52×15mm**
Yield strength, f_y (MPa)	255	474	455	483	471	1003
Tensile strength, f_u (MPa)	380	595	665	669	680	1079
Yield strain, ε_y	0.002	0.0021	0.0022	0.0022	0.0018	0.0042
Elongation at maximum force, ε_u	0.1448	0.1359	0.211	0.203	0.209	0.0091

Table 3 Main characteristics of reinforcement and confinement in tested beams

ID	f_c **(MPa)**	***Effective depth, d* (mm)**	***x/d***	***Flexural bars* (mm)**	ρ	***Confinement at midspan***	ρ_v
B50-1-C	54.5	119	0.53	2Ø10+2Ø12	0.0306	None	-
B50-1-40	54.5	119	0.53	2Ø10+2Ø12	0.0306	Straps/40mm	0.0893
B50-1-20	54.5	119	0.53	2Ø10+2Ø12	0.0306	Straps/20mm	0.1461
B50-2-C	51.1	113	0.56	2Ø8+2Ø16	0.0447	None	-
B50-2-40	51.1	113	0.56	2Ø8+2Ø16	0.0447	Straps/40mm	0.0893
B50-2-20	51.1	113	0.56	2Ø8+2Ø16	0.0447	Straps/20mm	0.1461
B80-1-C	79.6	119	0.62	2Ø10+2Ø12	0.0306	None	-
B80-1-30	79.6	119	0.62	2Ø10+2Ø12	0.0306	Straps/30mm	0.0665
B80-1-15	79.6	119	0.62	2Ø10+2Ø12	0.0306	Straps/15mm	0.1044
B80-2-C	78.8	113	0.65	2Ø8+2Ø16	0.0447	None	-
B80-2-30	78.8	113	0.65	2Ø8+2Ø16	0.0447	Straps/30mm	0.0665
B80-2-15	78.8	113	0.65	2Ø8+2Ø16	0.0447	Straps/15mm	0.1044

Table 4 Relevant test results from tested beams

ID	First crack (kN)	P_{max} (kN)	δ (mm)	ΔP_{max} (%)	$\Delta\delta$ (%)	δ_{-20} (mm)	δ_{-20}/δ (-)	Total number of cracks	Average crack spacing (mm)	Steel strain at failure (με)	Strap strain at failure (με)	Concrete strain at failure (με)	$P_{max,t}$ (kN) by *fib* Model Code (2013)	$\Delta P_{max,t}$ (%)
B50-1-C	10.0	46.0	23.0	-	-	-	0	28	65	1805	-	2330[b]	43.4	-
B50-1-20	10.0	50.0	30.0	+9	+30	48.0	1.60	19	115	10960	1375	2605	44.9	+3
B50-1-40	10.0	49.4	32.5	+7	+41	47.4	1.46	21	105	22575	1080	1825	44.1	+2
B50-2-C	10.0	36.0	22.6	-	-	-	0	24	65	3290	-	2610	54.3	-
B50-2-20	8.0	43.9	27.7	+22	+23	62.6	2.26	18	115	1750	970	3150	56.7	+5
B50-2-40	10.0	43.8	27.1	+22	+20	48.6	1.79	20	115	15620	545	2970	55.3	+2
B80-1-C	8.0	60.2	25.6	-	-	-	0	28	65	4320	-	1760	46.0	-
B80-1-15	8.0	65.3	35.5	+8	+39	60.4	1.70	28	65	-[a]	-[a]	-[a]	46.9	+2
B80-1-30	6.0	63.8	32.6	+6	+27	39.0	1.20	21	110	29795	190	2500	46.4	+1
B80-2-C	8.0	70.5	33.3	-	-	-	0	28	65	4310	-	2015	58.5	-
B80-2-15	8.0	66.8	33.0	-5	-1	55.6	1.68	22	110	40895	60	3035	60.0	+3
B80-2-30	6.0	67.7	34.0	-4	+2	43.1	1.27	26	100	16455	100	3385	59.2	+1

[a] Strain gauge readings not recorded by data logger
[b] Failure of strain gauge occurred before failure of beam

Figures

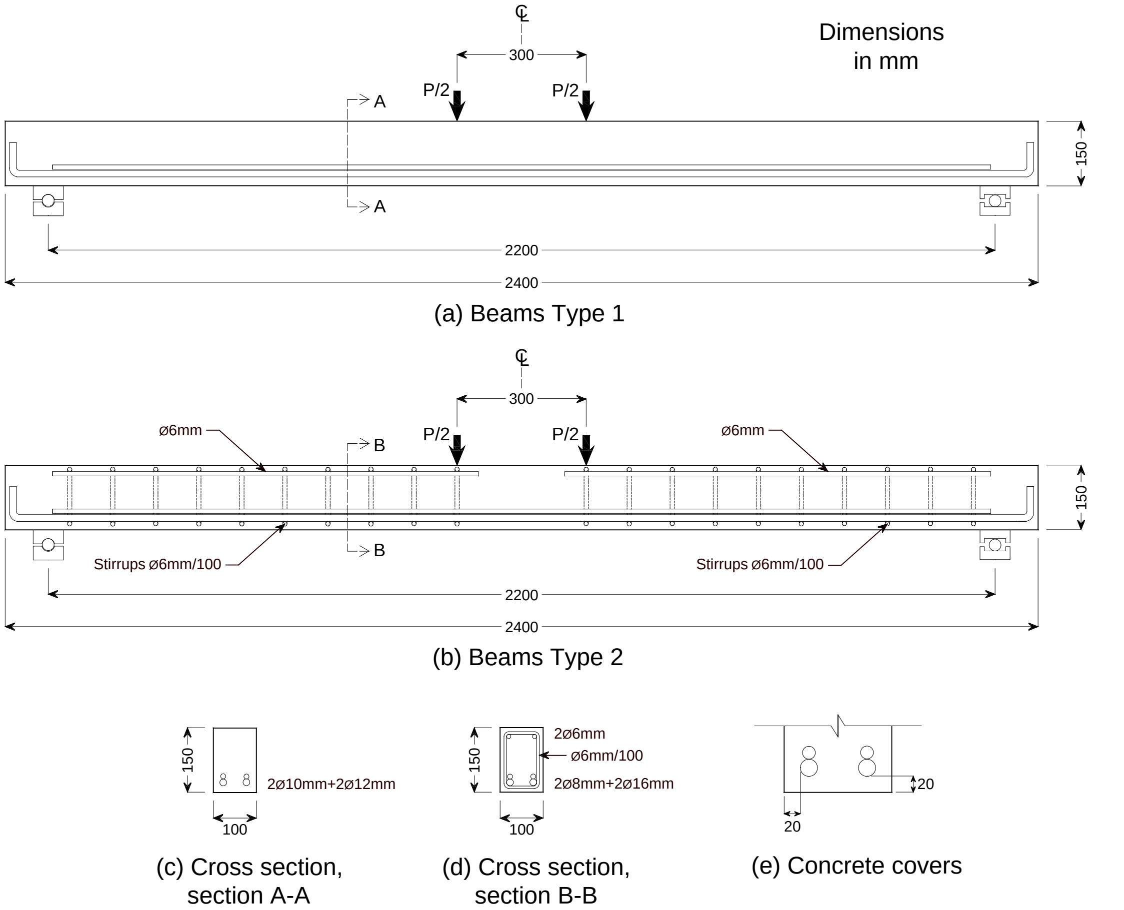

Figure 1 Beam specimens (a) Type 1, (b) Type 2, (c) Section A-A, (d) Section B-B, and (e) concrete covers

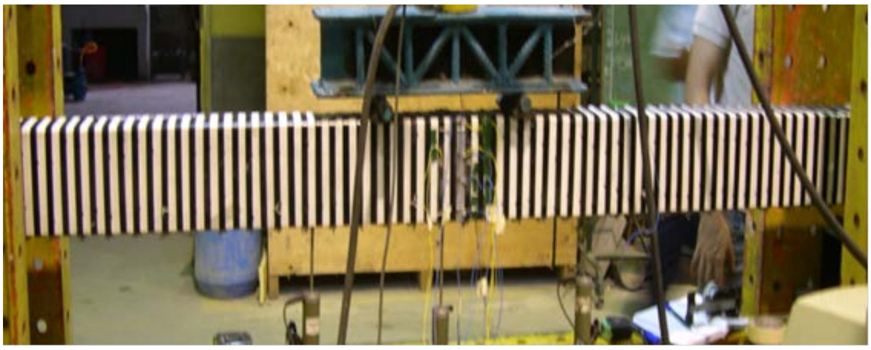

Figure 2 Final view of a typical HSC beam after strapping using the SSTT (beam B80-1-15)

Figure 3 View of self-regulated clips

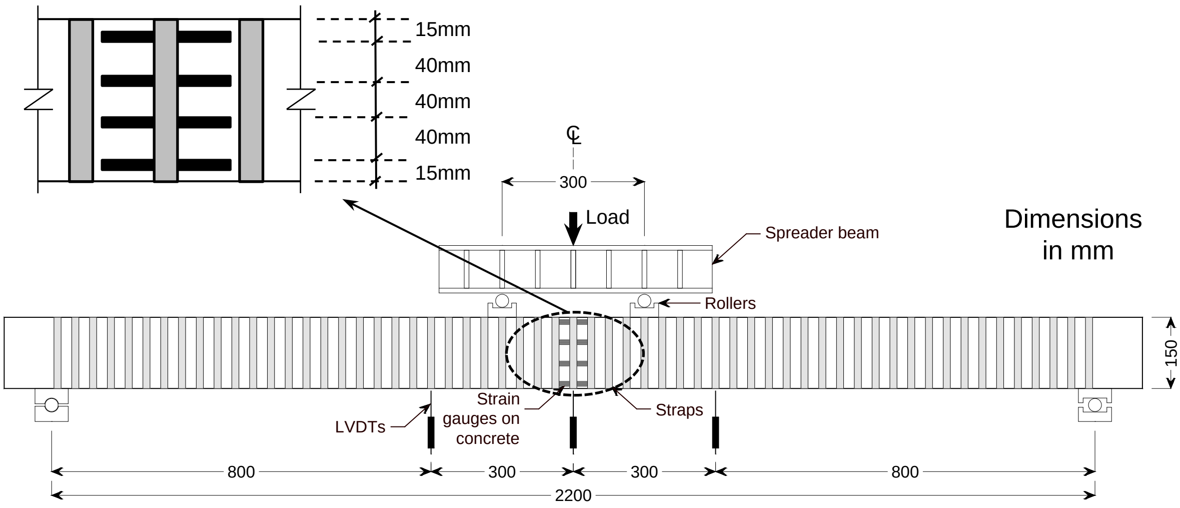

Figure 4 Typical set-up and instrumentation used during the tests

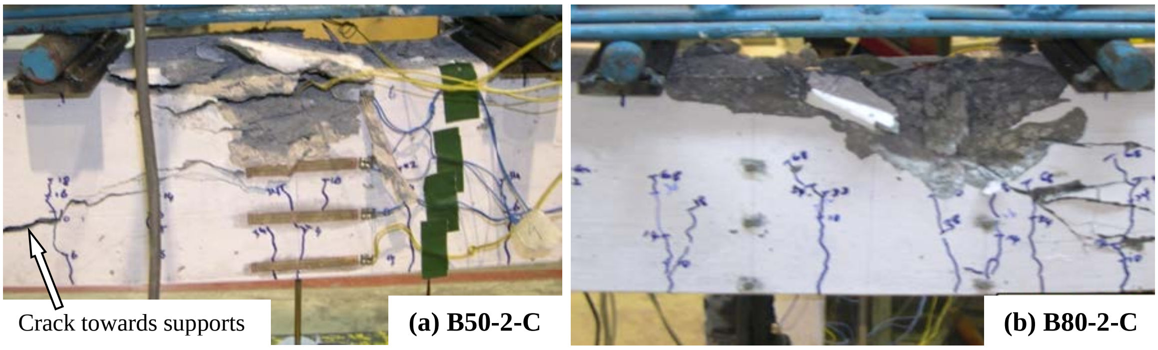

Figure 5 Typical failure of unconfined control beams

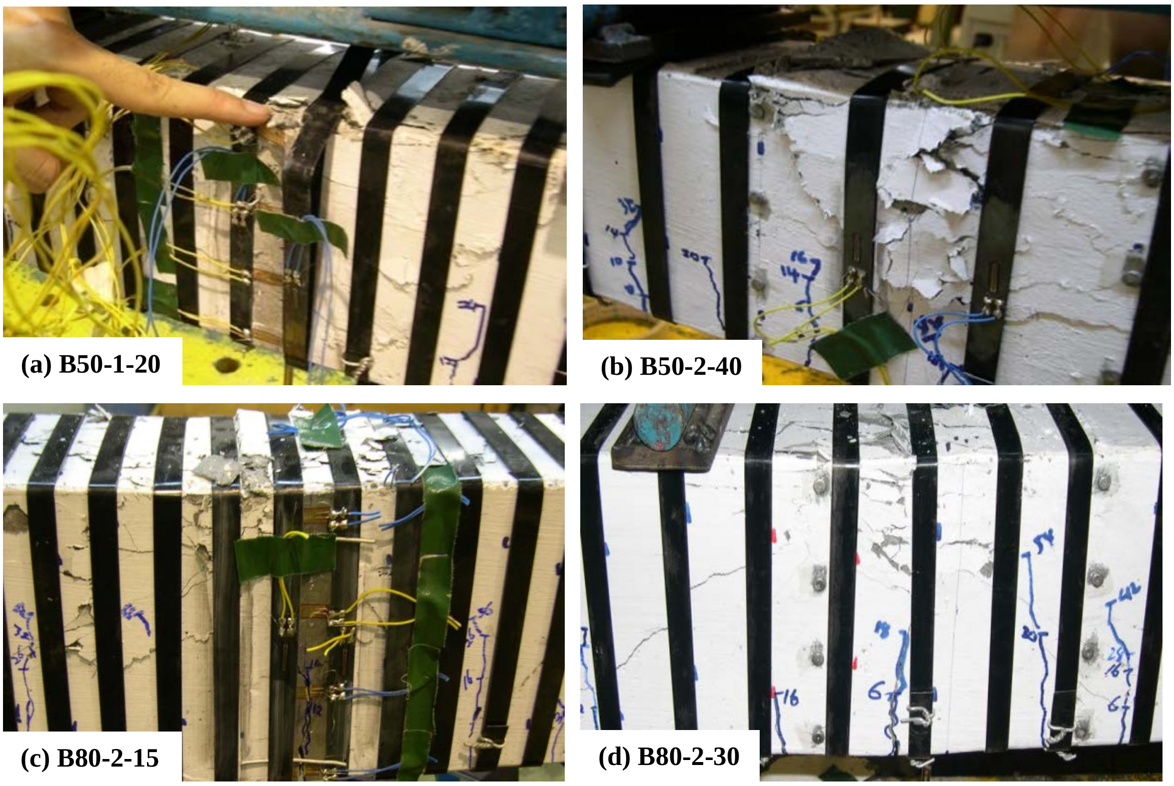

Figure 6 Typical failures at midspan of SSTT-confined beams

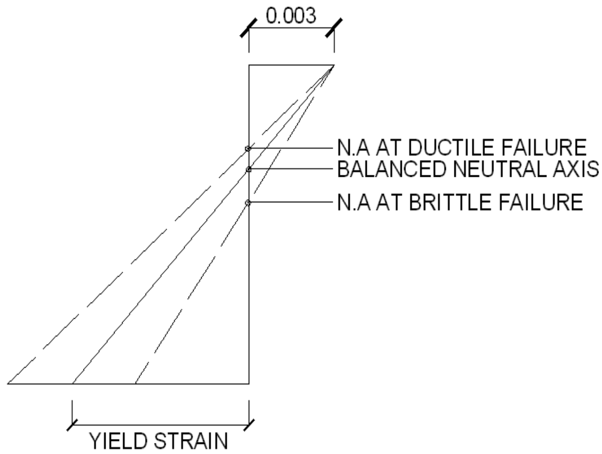

Figure 7 Strain distribution to explain failure modes in a member subjected to pure flexure

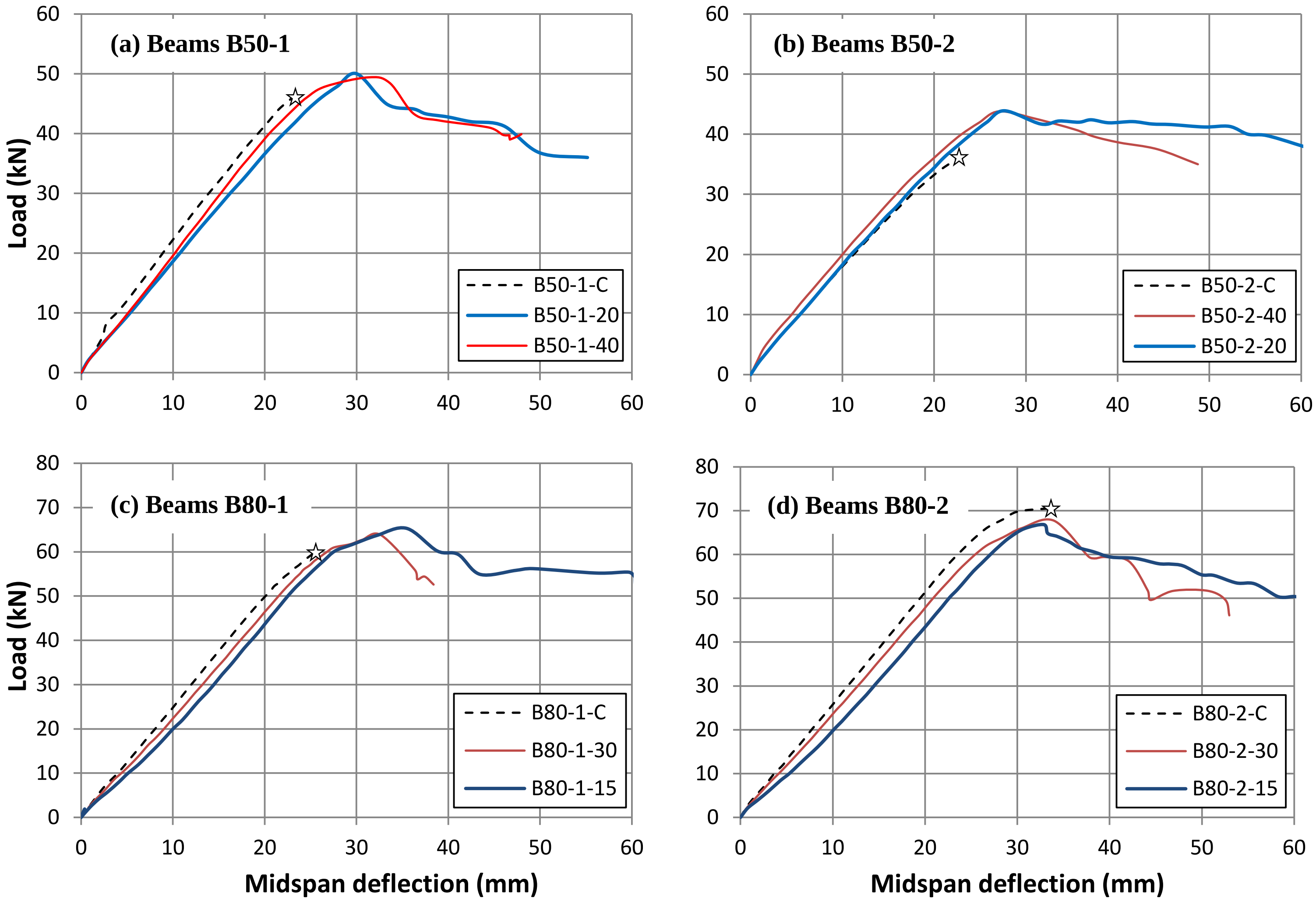

Figure 8 Load-midspan deflection for tested beams

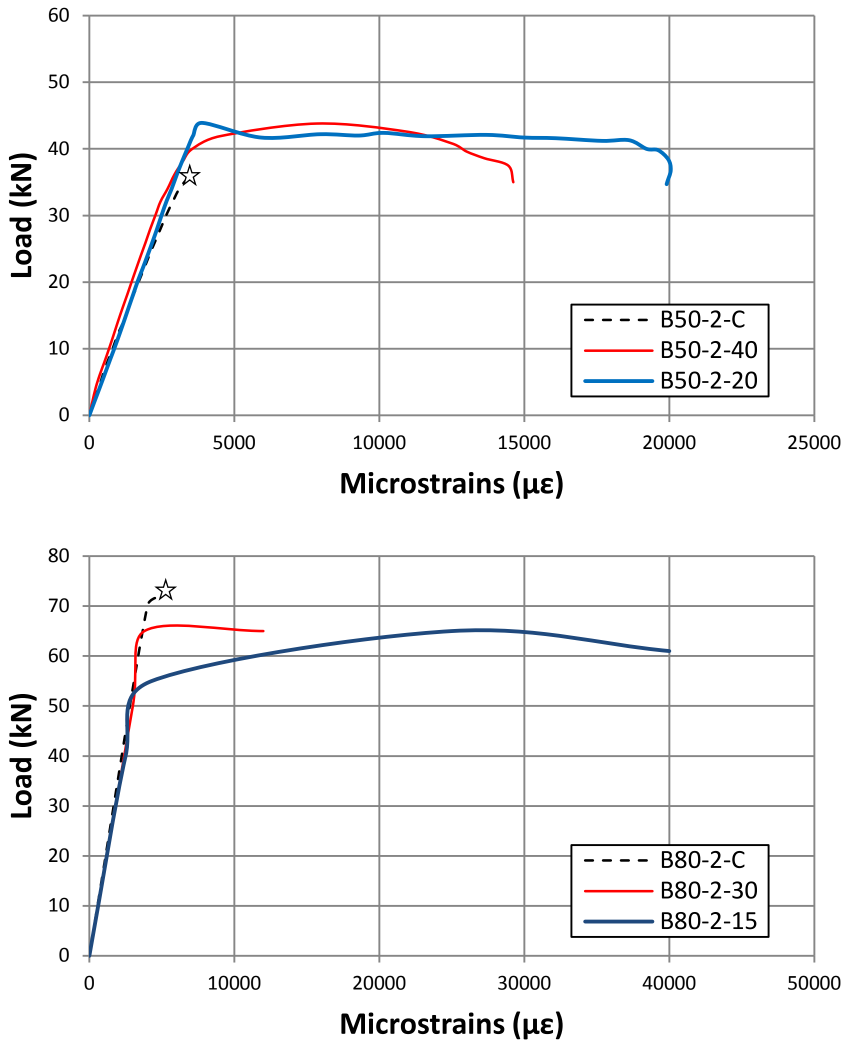

Figure 9 Typical load vs strain in flexural reinforcement

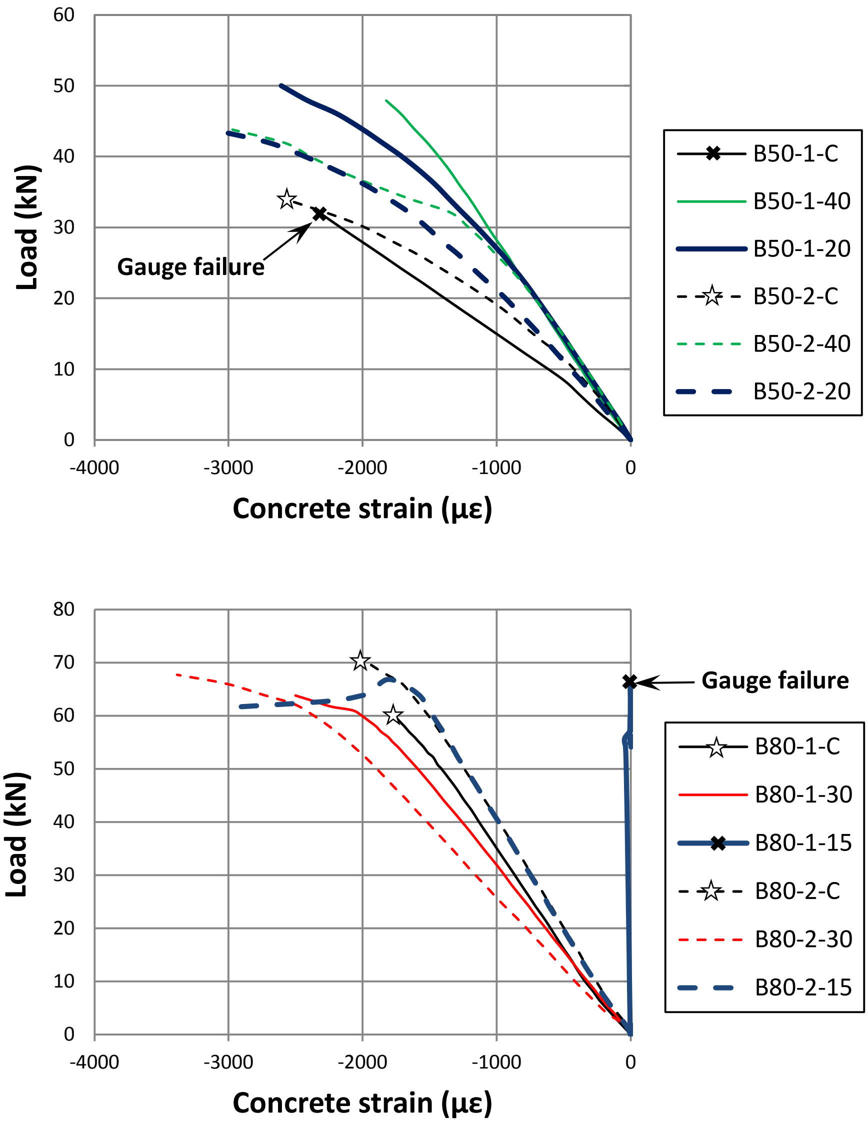

Figure 10 Development of strains in concrete subjected to compression at midspan